

Direct Joining of a Heterogeneous Pair of Supramolecular Nanotubes and Reaction Control of a Guest Compound by Transportation in the Nanochannels

Naohiro Kameta* and Wuxiao Ding

Nanomaterials Research Institute, Department of Materials and Chemistry, National Institute of Advanced Industrial Science and Technology (AIST), Tsukuba Central 5, 1-1-1 Higashi, Tsukuba, Ibaraki 305-8565, Japan

E-mail: n-kameta@aist.go.jp

Received: February 26, 2019; Accepted: March 13, 2019; Web Released: April 18, 2019



Naohiro Kameta

Naohiro Kameta received his PhD (2002) in Analytical Chemistry from Ibaraki University and then did postdoctoral research at Utsunomiya University and Japan Science and Technology Agency (JST, CREST-SORST). Since 2008, he has worked at AIST, where he is currently a senior researcher developing interfacial nanomaterials based on supramolecular and colloidal chemistry. He has received an Award for Encouragement of Research in Polymer Science from the Society of Polymer Science, Japan, and an Award for Encouragement of Research in Analytical Chemistry from the Japan Society for Analytical Chemistry.

Abstract

Four novel amino-acid lipids were synthesized and then self-assembled in water to produce four different types of supramolecular nanotubes. The nanotubes consisted of a single monolayer of amino-acid lipids packed in parallel and had similar inner diameters and membrane wall thicknesses but dissimilarly charged surfaces. Mixing of nanotubes that had cationic exterior surfaces with nanotubes that had anionic exterior surfaces resulted in aggregation of the nanotubes. In contrast, mixing of nanotubes with cationic interior surfaces and nanotubes with anionic interior surfaces resulted in end-to-end joining of the two types of nanotubes via electrostatic attractions at the open ends to form heterogeneous nanotubes. Time-lapse fluorescence microscopy confirmed that a fluorophore could be transported through the heterogeneous nanotubes, which had alternating acidic and basic nanochannel segments. In addition, acid–base reactions of the fluorophore could be precisely controlled during transport. This nanotube-joining technique should be useful not only for the construction of multifunctional hybrid nanotubes but also for the production of nanoreactors for chemical/biological reactions and nano-devices for analysis and separation.

Keywords: Supramolecular nanotube | Self-assembly | Amino-acid lipids

1. Introduction

Supramolecular nanotubes,¹ which can be formed by self-assembly of rationally-designed synthetic lipids and amphiphilic molecules in the liquid phase, have the following unique

morphological and structural features: (i) a perfect one-dimensional morphology, (ii) distinct, functionalizable inner and outer surfaces, and (iii) nanochannels with tunable diameters. The one-dimensional morphology is advantageous for electronic and optical applications, when component molecules are integrated with dye moieties, because the dye moieties packed in a highly ordered manner within the membrane walls of the nanotubes exhibit high-speed charge transport, long-lasting charge separation, efficient energy transfer, and light harvesting.^{2–7} The functionalizable surfaces permit selective chemical and biological modifications and complexation of metals on the surfaces, and functionalized nanotubes can serve as sensing platforms,^{8,9} reusable and recyclable solid catalysts with large specific surface areas,^{10–12} and self-propelled micro-machines acting as scavengers for viruses and bacteria.¹³ The tunability of the nanochannel diameter is important for biological (e.g., pharmaceutical and medical) and materials science applications. For example, the nanochannels can be utilized as templates not only to produce conformationally controlled polymers^{14–17} but also to fabricate nanoparticles, nanorods, nanocoils, and nanotubes from metals or other inorganic materials.^{10,18–21} Nanochannels are also useful for separating peptides,²² stabilizing enzymes,^{23,24} accelerating DNA duplex formation, and refolding denatured proteins.^{25–27} Furthermore, the nanochannels can store and release drugs in response to external stimuli, including environmental changes.^{28,29}

The recent development of methods for stepwise self-assembly and living supramolecular polymerization³⁰ of two components has permitted the construction of hybrid nanotubes in which two different nanotube segments are joined end-to-

end.^{31–33} For example, Fukushima and Aida et al. have succeeded in fabricating a heterojunction between two semiconducting nanotube segments by self-assembly of one graphene-like molecule to form a seed nanotube that facilitates self-assembly of another graphene-like molecule.³¹ The dissimilar nanotube segments can communicate electrically and energetically with each other over the heterojunction interface. However, direct joining of heterogeneous nanotube segments formed in advance by self-assembly of their respective components has been reported to a limited degree,^{34,35} although uniaxial stacking of toroidal- and barrel-like nanostructures acting as homogeneous nanotube segments has been observed during the formation and elongation of natural and artificial bionanotubes^{36–40} and supramolecular nanotubes.^{41–44}

Herein we describe direct joining of supramolecular nanotubes that have similar diameters but dissimilarly charged surfaces and that are formed by self-assembly of novel amino-acid lipids. Specifically, nanotubes with cationic interior surfaces were joined to nanotubes with anionic interior surfaces by means of an electrostatic attraction between the open ends of the nanotubes. Time-lapse fluorescence microscopy revealed that acid–base reactions of a fluorophore could be controlled during transport of the fluorophore through the resulting heterogeneous nanotubes, which had alternating acidic and basic nanochannel segments.

2. Experimental

2.1 Synthesis and Characterization of Amino-Acid Lipids. The syntheses of the amino-acid lipids are shown schematically in Supporting Information.

NH₂-Phe-C₁₁-Gly: ¹H NMR (500 MHz, DMSO-*d*₆, 25 °C): δ = 7.97 (t, *J* = 5.5 Hz, 1H; NH), 7.78 (br, 1H; NH), 7.75 (t, *J* = 5.5 Hz, 1H; NH), 7.26 (t, *J* = 7.0 Hz, 3H; -CH-CH₂-C₆H₅), 7.18 (d, *J* = 7.0 Hz, 2H; -CH-CH₂-C₆H₅), 3.61 (d, *J* = 6.0 Hz, 2H; HN-CH₂-C=O), 3.09–2.97 (overlap, 5H; HN-CH₂-CH₂, HN-CH₂-CH₃, -CH-CH₂-C₆H₅), 2.87 (dd, *J* = 5.5, 13 Hz, 1H; -CH-CH₂-C₆H₅), 2.60 (dd, *J* = 7.5, 13 Hz, 1H; -CH-CH₂-C₆H₅), 2.11 (t, *J* = 7.5 Hz, 2H; CH₂-CH₂-C=O), 1.48 (m, 2H; -CH₂-), 1.32 (m, 2H; -CH₂-), 1.24 (m, 14H; -CH₂-), 0.99 (t, *J* = 7.0 Hz, 3H; HN-CH₂-CH₃). ESI-MS (cationic mode) *m/z*: 447.3 [M + H]⁺. Anal. calculated for C₂₅H₄₂N₄O₃: C 62.16, H 8.97, N 11.60; found: C 62.08, H 8.99, N 11.61.

Gly-C₁₁-Phe-COOH: ¹H NMR (500 MHz, DMSO-*d*₆, 25 °C): δ = 7.91 (t, *J* = 8.5 Hz, 1H; NH), 7.81 (br, 1H; NH), 7.62 (t, *J* = 6.0 Hz, 1H; NH), 7.22 (m, 5H; -CH-CH₂-C₆H₅), 4.44 (m, 1H; -CH-CH₂-C₆H₅), 3.62 (d, *J* = 6.0 Hz, 2H; HN-CH₂-C=O), 3.13–3.00 (overlap, 3H; HN-CH₂-CH₂, -CH-CH₂-C₆H₅), 2.84 (dd, *J* = 9.5, 13 Hz, 1H; -CH-CH₂-C₆H₅), 2.16 (m, 2H; CH₃-CH₂-C=O), 2.03 (t, *J* = 7.5 Hz, 2H; CH₂-CH₂-C=O), 1.49 (m, 2H; -CH₂-), 1.39 (m, 2H; -CH₂-), 1.24 (m, 14H; -CH₂-), 0.99 (t, *J* = 7.5 Hz, 3H; CH₃-CH₂-C=O). ESI-MS (anionic mode) *m/z*: 474.3 [M – H][–]. Anal. calculated for C₂₆H₄₁N₃O₅: C 65.66, H 8.69, N 8.83; found: C 65.68, H 8.59, N 8.81.

NH₂-Gly-C₁₁-Phe: ¹H NMR (500 MHz, DMSO-*d*₆, 25 °C): δ = 7.97 (d, *J* = 8.5 Hz, 1H; NH), 7.91 (t, *J* = 5.5 Hz, 1H; NH), 7.81 (t, *J* = 5.5 Hz, 1H; NH), 7.76 (t, *J* = 5.5 Hz, 1H; NH), 7.25–7.15 (m, 5H; -CH-CH₂-C₆H₅), 4.44 (m, 1H; -CH-CH₂-C₆H₅), 3.68 (d, *J* = 6.0 Hz, 2H; HN-CH₂-C=O), 3.11 (s, 1H; H₂N-CH₂-C=O), 3.09–3.01 (overlap, 4H; HN-CH₂-CH₂,

HN-CH₂-CH₃), 2.93 (dd, *J* = 5.0, 13 Hz, 1H; -CH-CH₂-C₆H₅), 2.72 (dd, *J* = 9.5, 13 Hz, 1H; -CH-CH₂-C₆H₅), 2.01 (t, *J* = 7.5 Hz, 2H; CH₂-CH₂-C=O), 1.49 (m, 2H; -CH₂-), 1.34 (m, 2H; -CH₂-), 1.24 (m, 14H; -CH₂-), 0.96 (t, *J* = 7.0 Hz, 3H; HN-CH₂-CH₃). ESI-MS (cationic mode) *m/z*: 504.4 [M + H]⁺. Anal. calculated for C₂₇H₄₅N₃O₄: C 64.38, H 9.01, N 13.90; found: C 64.01, H 9.19, N 13.81.

Phe-C₁₁-Gly-COOH: ¹H NMR (500 MHz, DMSO-*d*₆, 25 °C): δ = 12.4 (s, 1H; -COOH), 8.09 (t, *J* = 6.0 Hz, 1H; NH), 8.04 (t, *J* = 6.0 Hz, 1H; NH), 7.96 (d, *J* = 9.0 Hz, 1H; NH), 7.89 (t, *J* = 6.0 Hz, 1H; NH), 7.25–7.15 (m, 5H; -CH-CH₂-C₆H₅), 4.44 (m, 1H; -CH-CH₂-C₆H₅), 3.74 (d, *J* = 6.0 Hz, 2H; HN-CH₂-C=O), 3.70 (d, *J* = 6.0 Hz, 2H; HN-CH₂-C=O), 3.17–2.89 (overlap, 3H; HN-CH₂-CH₂, -CH-CH₂-C₆H₅), 2.73 (dd, *J* = 9.5, 13 Hz, 1H; -CH-CH₂-C₆H₅), 2.11 (t, *J* = 7.5 Hz, 2H; CH₂-CH₂-C=O), 2.03 (q, *J* = 7.5 Hz, 2H; CH₃-CH₂-C=O), 1.48 (m, 2H; -CH₂-), 1.32 (m, 2H; -CH₂-), 1.24 (m, 14H; -CH₂-), 0.87 (t, *J* = 7.5 Hz, 3H; CH₃-CH₂-C=O). ESI-MS (anionic mode) *m/z*: 531.2 [M – H][–]. Anal. calculated for C₂₈H₄₄N₄O₆: C 63.13, H 8.33, N 10.52; found: C 63.18, H 8.39, N 10.51.

2.2 Observation of Nanotube Morphology. Aqueous dispersions of nanotubes were dropped onto a carbon grid, negatively stained with 0.2 wt% phosphotungstate in 90:10 (v/v) water/CH₃OH (adjusted to pH 7 with NaOH), and observed with a transmission electron microscope (H-7000, Hitachi) at 75 kV. The nanotube xerogel was observed with a scanning electron microscope (S-4800, Hitachi) at 15 kV.

2.3 Analysis of Nanotube Structure. The pH of the aqueous dispersions of (–)-out-nanotube and (–)-in-nanotube was adjusted to 4.2, which led to the protonation of the carboxyl groups on the outer or inner surfaces of both nanotubes, to clearly observe the amide-I and -II bands related to the intermolecular hydrogen bond interaction. All nanotubes were lyophilized and analyzed with a Fourier transform infrared spectrometer (FT-620, JASCO) operated at 4 cm^{–1} resolution and equipped with an unpolarized beam, an attenuated total reflection accessory system (Diamond MIRacle, horizontal attenuated total reflection accessory with a diamond crystal prism, PIKE Technologies), and a mercury-cadmium telluride detector. The zeta potentials of the surfaces of the nanotubes dispersed in water were measured with a Malvern Zetasizer Nano ZS system.

2.4 Dynamic Observation of a Fluorophore in the Nanochannels. The transport of the fluorophore CypHer5 (GE Healthcare) in the nanochannels of the heterogeneous nanotubes was monitored with an inverted microscope (IX71; Olympus) equipped with a CCD camera (ORCA-ER; Hamamatsu). The excitation optical source consisted of a high-pressure mercury lamp (100 W, BH2-REL-T3; Olympus). Fluorescence detection was optimized by means of an appropriate mirror unit (U-DM-CY5; Olympus). Time-lapse fluorescence microscopic images were recorded on a PC with the Aquacosmos system (Hamamatsu). The measurement interval was set to 10 ms.

3. Results and Discussion

3.1 Construction of Nanotubes with Dissimilarly Charged Surfaces and Similar Diameters. As previously reported

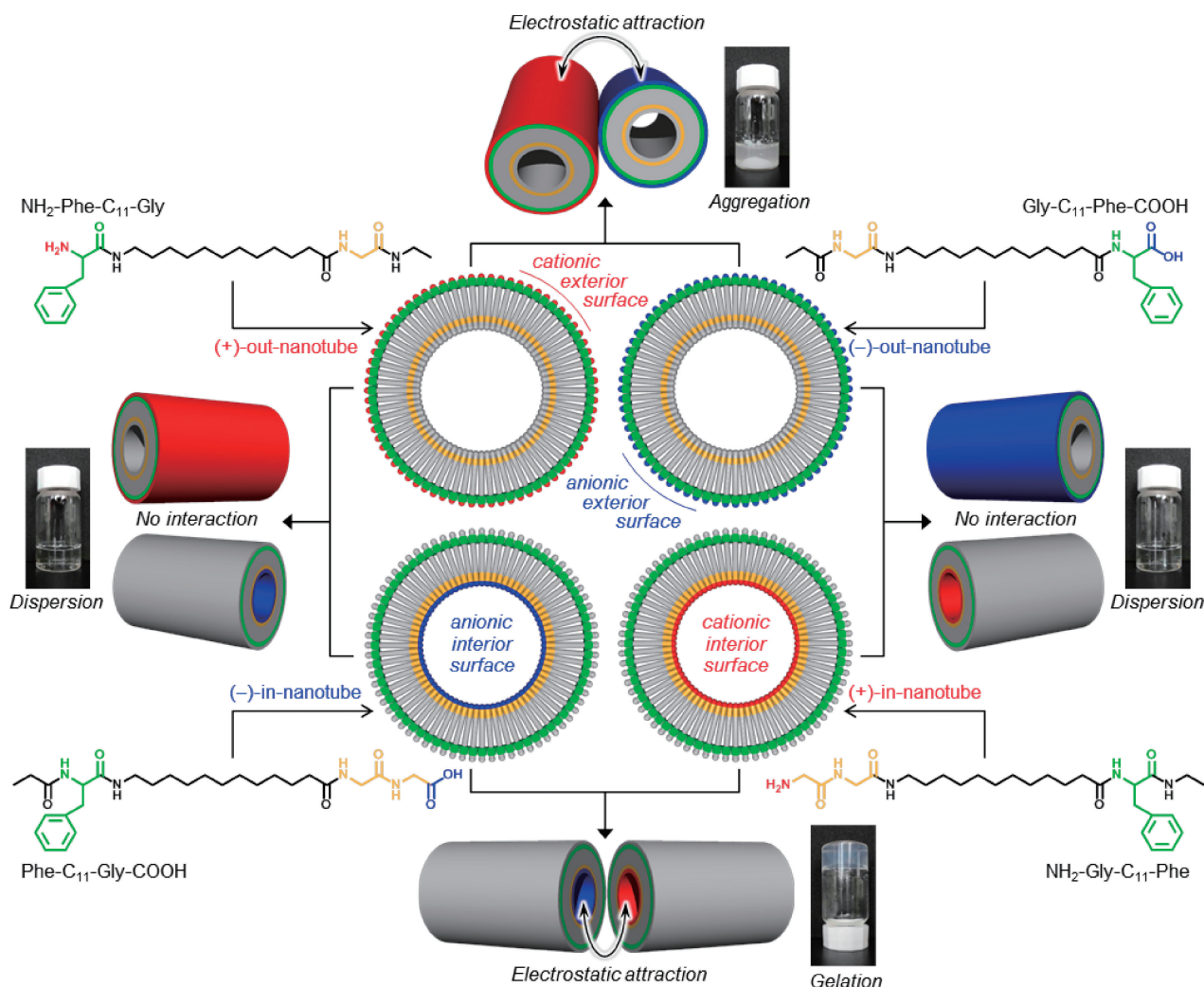


Figure 1. Chemical structures of amino-acid lipids, schematic representation of nanotubes consisting of a single monolayer formed by self-assembly of the amino-acid lipids, and photographs showing the results of mixing clear aqueous dispersions of pairs of nanotube types.

by our group, synthetic glycolipids composed of an oligomethylene spacer capped on one end with a large glucose headgroup and on the other with a small amino or carboxyl headgroup self-assemble in water to form nanotubes.²⁹ The nanotubes consist of monolayer membranes in which the glycolipids pack in parallel. The nanotubes have different exterior and interior surfaces; specifically, the exterior is covered with the nonionic glucose headgroups and the interior with the cationic amino headgroups or anionic carboxyl headgroups. However, we have found it difficult to prepare and combine nanotubes with dissimilarly charged surfaces and similar diameters (both outer and inner). Especially, we have never succeeded in control of outer diameters, i.e., monolayer membrane wall thicknesses, which strongly depend on not only the stacking number of the monolayer membrane but also the molecular length of the used glycolipids and the tilting angle of the glycolipids within the single monolayer membrane.

In this study, with the goal of preparing four types of nanotubes with cationic or anionic exterior or interior surfaces and

similar diameters (both outer and inner), we designed and synthesized four new amino-acid lipids (Scheme S1–S4). These lipids, designated **NH₂-Phe-C₁₁-Gly**, **Gly-C₁₁-Phe-COOH**, **NH₂-Gly-C₁₁-Phe**, and **Phe-C₁₁-Gly-COOH**, have an L-phenylalanine derivative as a large headgroup, a glycine derivative as a small headgroup, and a 12-aminododecanoic acid linker connecting the two headgroups (Figure 1).

The nanotubes were generated as follows. Each amino-acid lipid (10 mg) was dispersed in deionized water (10 mL) by refluxing for 5 min and was then rapidly cooled in an ice bath. Transmission electron microscopy revealed that all the amino-acid lipids formed only nanotubes (Figure 2a–d). The four types of nanotubes had similar outer diameters (22 nm), inner diameters (16 nm), and membrane wall thicknesses (3 nm). The fact that the membrane wall thicknesses were comparable to the extended molecular lengths (3.2–3.6 nm) of the amino-acid lipids indicates that the nanotubes consisted of single monolayer membranes composed of the lipids.²⁹ Infrared spectroscopy confirmed that the molecular packing of the lipids within

the monolayer membranes was similar for the four types of nanotubes. Specifically, the absence of obvious differences in the amide-I and -II bands reflected the strength of intermolecular hydrogen bonding (Figure S1). The spectra showed two peaks, at 1420 and 1026 cm^{-1} , that were assignable to the CH deformation and skeletal vibration bands of the glycine moieties of the lipids, suggesting that the lipids in the nanotubes formed a pseudo-polyglycine-II-type hydrogen bond network (Figure S1).^{45–48} The $\gamma(\text{CH}_2)$ rocking vibration produced a single sharp peak at 719 cm^{-1} , which indicates that the subcellular structure (lateral chain packing) of the oligomethylene spacers of the lipids in the nanotubes was triclinic parallel ($T_{//}$).⁴⁹ The specific intermolecular hydrogen bonding and the subcell structure ensured the parallel molecular packing of the lipids within the monolayer membrane.

The above-described results indicated that for all the nanotubes, the L-phenylalanine-derived headgroups were on the exterior surfaces, and the glycine-derived headgroups were on the interior surfaces (Figure 1). The zeta potential of the nanotubes formed from **NH₂-Phe-C₁₁-Gly** (designated as (+)-out-nanotubes) in a water dispersion was approximately 55 mV (Figure S2), which is consistent with the amino groups of the L-phenylalanine headgroups being on the exterior surface of the nanotubes. In contrast, the nanotubes formed from **Gly-C₁₁-Phe-COOH** ((-)-out-nanotubes) had a negative zeta potential (-78 mV) derived from the carboxyl groups of the L-phenylalanine headgroups on the outer surfaces. The zeta potentials of the nanotubes formed from **NH₂-Gly-C₁₁-Phe** and **Phe-C₁₁-Gly-COOH** ((+)-in-nanotubes and (-)-in-nanotubes, respectively) were much smaller than those of the above-mentioned nanotubes (Figure S2). The smaller zeta potentials are ascribable to the fact that the amino and carboxyl groups of the glycine headgroups on the interior surfaces of the (+)-in-nanotubes and (-)-in-nanotubes had less contact with the bulk solution (Figure 1).

3.2 Joining of a Heterogeneous Pair of Nanotubes via Electrostatic Attraction. Mixing of clear aqueous dispersions of (+)-out-nanotubes and (-)-out-nanotubes led to the formation of a cloudy dispersion (Figure 1, top photograph), whereas mixing of aqueous dispersions of (+)-out-nanotubes and (-)-in-nanotubes or (-)-out-nanotubes and (+)-in-nanotubes resulted in clear dispersions (Figure 1, left and right photographs, respectively). The formation of the cloudy dispersion in the former case suggests that electrostatic attraction between the cationic exterior surfaces of the (+)-out-nanotubes and the anionic exterior surfaces of the (-)-out-nanotubes led to aggregation. In contrast, in the other two pairings, there were no attractive interactions between the nanotubes. Transmission electron microscopy confirmed that mixing the pairs of nanotubes did not affect their morphology, diameter, or length.

In contrast, mixing clear aqueous dispersions of (+)-in-nanotubes and (-)-in-nanotubes resulted in hydrogel formation (Figure 1, bottom photograph). Scanning electron microscopy of the lyophilized hydrogel (xerogel) revealed a network of entangled nanotubes (Figure 2e). These nanotubes were several micrometers long, which is much longer than the original nanotubes prior to mixing (~300 nm, Figure 2c,d and Figure S3). Because this elongation was not observed for any of the other pairs of nanotubes, we attributed it to end-to-end joining of the

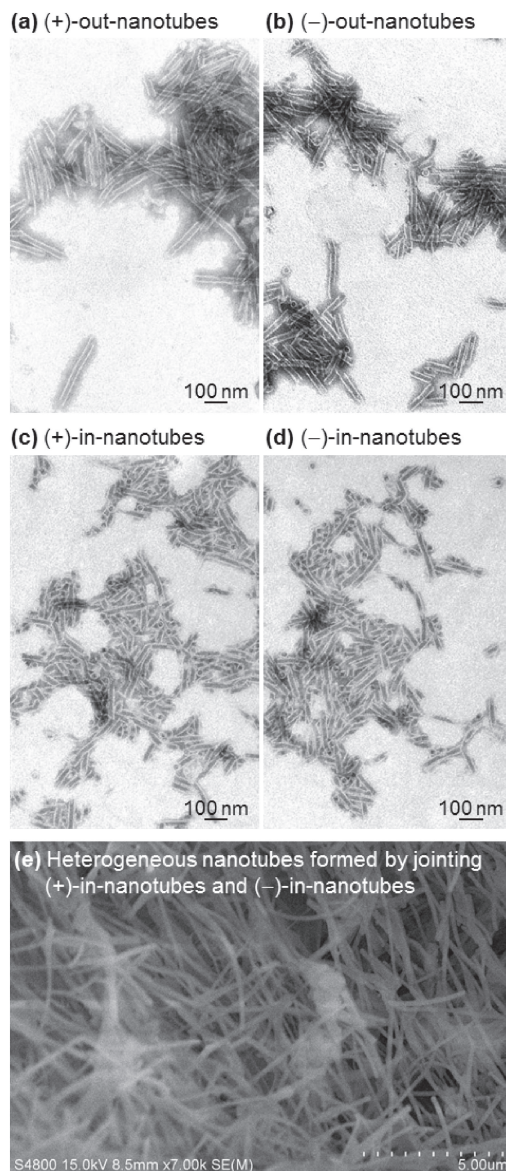


Figure 2. (a–d) Transmission electron micrographs of the four types of nanotubes. The nanotube channels were negatively stained with 2 wt% phosphotungstate. (e) Scanning electron micrograph of the xerogel obtained by joining the (+)-in-nanotubes and (-)-in-nanotubes and subsequent lyophilization.

(+)-in-nanotubes and (-)-in-nanotubes to form long heterogeneous nanotubes.

To elucidate the joining of the nanotubes, we mixed (-)-in-nanotubes containing *cis*-diamine-Pt(II) complexed to the interior carboxyl groups⁵⁰ with vacant (+)-in-nanotubes. Transmission electron microscopy clearly showed a single nanotube with nanochannel segments encapsulating the dark-colored Pt(II) complexes alternating with vacant nanochannel segments (Figure 3). At the interfaces between the open ends of the nanotubes, local electrostatic attractions between the cationic inner surfaces of the (+)-in-nanotubes and the anionic inner

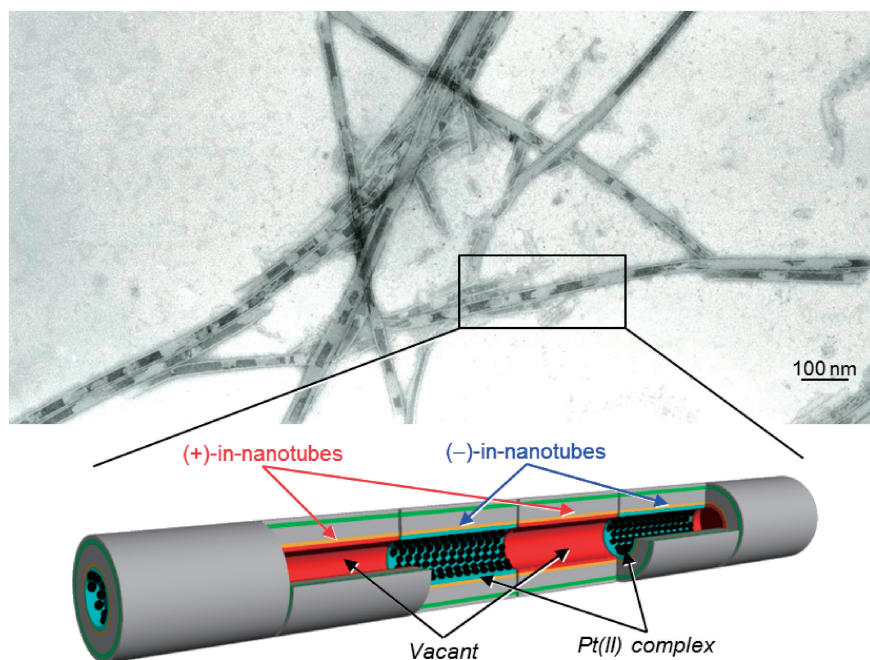


Figure 3. Transmission electron micrograph and schematic representation of heterogeneous nanotubes composed of Pt(II)-complex-containing (–)-in-nanotube segments joined end-to-end with vacant (+)-in-nanotube segments.

surfaces of the (–)-in-nanotubes induced joining of these two types of nanotubes.

3.3 Control of the Reactions of a Fluorophore during Transport through the Nanochannels. We speculated that the heterogeneous nanotubes formed by joining the (+)-in-nanotubes and (–)-in-nanotubes could be used to control acid–base reactions of compounds encapsulated in the alternating acidic and basic nanochannel segments. For the guest compound, we chose the pH-responsive fluorophore CypHer5,⁵¹ which fluoresces strongly at pH values lower than its pK_a (6.1) but emits no fluorescence under neutral or basic conditions.

Time-lapse fluorescence microscopy enabled us to visualize the encapsulation and transport of the CypHer5 in the heterogeneous nanotubes. To introduce an aqueous solution of the fluorophore into the nanochannels by capillary action,⁵² we first vacuum-dried the nanotubes to remove water from the nanochannels. Then we prepared an aqueous solution of CypHer5 containing 0.1 M NaCl to interrupt the electrostatic attraction between the fluorophore and the charged interior surfaces of the nanotubes. Upon addition of the nonfluorescent solution of CypHer5 at pH 7.4 to the vacuum-dried nanotubes on a glass plate, a bright fluorescent line appeared in the first segment of the nanotubes (segment 1 in Figure 4a), and as time passed, the line elongated in one direction (Figure 4b). A new bright fluorescent line appeared in segment 3, which is remote from segment 1 (Figure 4c,d). That is, at 40 s after addition of the CypHer5 to the nanotubes, there was a nonfluorescent segment (segment 2) between segments 1 and 3. As time passed, fluorescence developed in segment 5, whereas there was no fluorescence in segment 4 (Figure 4e,f). This unidirectional movement of the CypHer5 fluorescence corresponded to an event in

a single heterogeneous nanotube, suggesting that the heterojunction between the (+)-in-nanotubes and (–)-in-nanotubes was stable enough for smooth transport of the fluorophore. The encapsulated CypHer5 fluoresced during transport through the acidic nanochannels of the (–)-in-nanotubes, whereas no fluorescence was observed during transport through the basic nanochannels of the (+)-in-nanotubes (Figures 4a'–f'). Alternating protonation and deprotonation reactions of CypHer5 could be precisely controlled during transport of the fluorophore through the heterogeneous nanotubes.

4. Conclusion

We succeeded in directly joining two different types of nanotubes that had similar diameters but different surface charges. Electrostatic attraction between the open ends of the two types of nanotubes, which had cationic interior surfaces and anionic interior surfaces, respectively, led to end-to-end joining of the nanotubes. We also found that acid–base reactions of a fluorophore could be controlled during transport through the heterogeneous nanotubes, which had alternating acidic and basic nanochannel segments. This joining technique can be expected to be useful not only for the construction of multifunctional hybrid nanotubes but also for the production of nanoreactors and analytical nanodevices.

This work was supported by JSPS KAKENHI grant no. JP17H02726.

Supporting Information

Synthesis of amino-acid lipids, molecular packing analysis of nanotubes, zeta-potential and length-distribution measure-

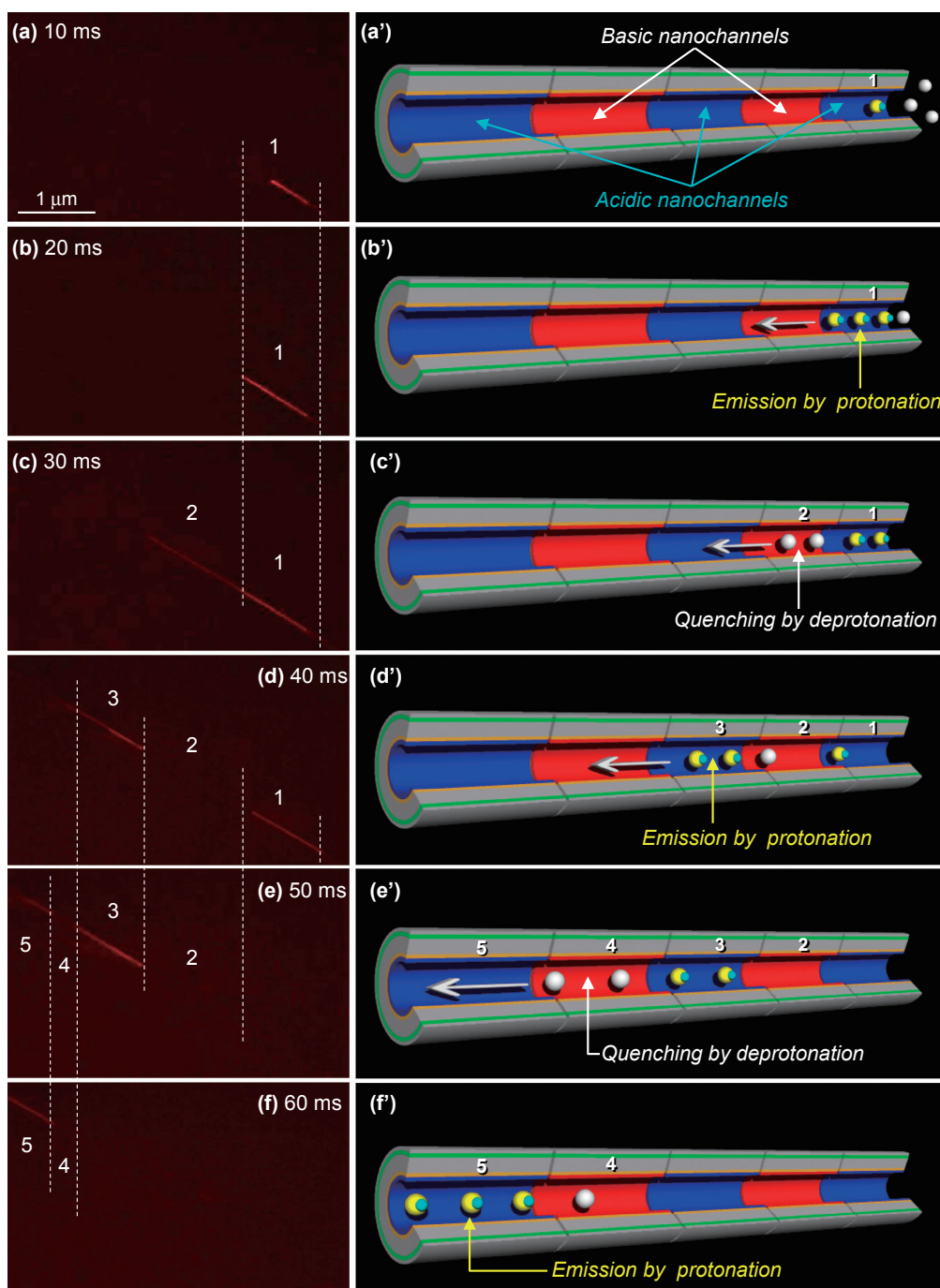


Figure 4. (a–f) Time-lapse fluorescence micrographs and (a'–f') schematic representation of CypHer5 transport through a heterogeneous nanotube 10–60 ms after addition of an aqueous solution of the fluorophore to vacuum-dried nanotubes on a glass plate.

ments of nanotubes. This material is available on <https://doi.org/10.1246/bcsj.20190046>.

References

- 1 T. Shimizu, *Bull. Chem. Soc. Jpn.* **2018**, *91*, 623.
- 2 H. Shao, J. Seifert, N. C. Romano, M. Gao, J. J. Helmus, C. P. Jaronec, D. A. Modarelli, J. R. Parquette, *Angew. Chem., Int. Ed.* **2010**, *49*, 7688.
- 3 T. Aida, E. W. Meijer, S. I. Stupp, *Science* **2012**, *335*, 813.
- 4 S. Sengupta, D. Ebeling, S. Patwardhan, X. Zhang, H. von Berlepsch, C. Böttcher, V. Stepanenko, S. Uemura, C. Hentschel, H. Fuchs, F. C. Grozema, L. D. A. Siebbeles, A. R. Holzwarth, L. Chi, F. Würthner, *Angew. Chem., Int. Ed.* **2012**, *51*, 6378.
- 5 S. Shoji, T. Ogawa, T. Hashishin, S. Ogasawara, H. Watanabe, H. Usami, H. Tamiaki, *Nano Lett.* **2016**, *16*, 3650.
- 6 N. Kameta, M. Aoyagi, M. Asakawa, *Chem. Commun.* **2017**, *53*, 10116.
- 7 F. Ishiwari, Y. Shoji, T. Fukushima, *Chem. Sci.* **2018**, *9*,

- 2028.
- 8 R. de la Rica, C. Pejoux, H. Matsui, *Adv. Funct. Mater.* **2011**, *21*, 1018.
- 9 L. Adler-Abramovich, E. Gazit, *Chem. Soc. Rev.* **2014**, *43*, 6881.
- 10 T. Shimizu, H. Minamikawa, M. Kogiso, M. Aoyagi, N. Kameta, W. Ding, M. Masuda, *Polym. J.* **2014**, *46*, 831.
- 11 J. Jiang, G. Ouyang, L. Zhang, M. Liu, *Chem.—Eur. J.* **2017**, *23*, 9439.
- 12 S. Wu, Y. Li, S. Xie, C. Ma, J. Lim, J. Zhao, D. S. Kim, M. Yang, D. K. Yoon, M. Lee, S. O. Kim, Z. Huang, *Angew. Chem., Int. Ed.* **2017**, *56*, 11511.
- 13 S. Kobayakawa, Y. Nakai, M. Akiyama, T. Komatsu, *Chem.—Eur. J.* **2017**, *23*, 5044.
- 14 K. Sada, M. Takeuchi, N. Fujita, M. Numata, S. Shinkai, *Chem. Soc. Rev.* **2007**, *36*, 415.
- 15 M. Numata, S. Shinkai, *Chem. Commun.* **2011**, *47*, 1961.
- 16 W. Ding, S. A. Chechetka, M. Masuda, T. Shimizu, M. Aoyagi, H. Minamikawa, E. Miyako, *Chem.—Eur. J.* **2016**, *22*, 4345.
- 17 N. Kameta, M. Masuda, T. Shimizu, *Chem. Commun.* **2016**, *52*, 1346.
- 18 O. Carny, D. E. Shalev, E. Gazit, *Nano Lett.* **2006**, *6*, 1594.
- 19 D. M. Eisele, H. v. Berlepsch, C. Böttcher, K. J. Stevenson, D. A. Vanden Bout, S. Kirstein, J. P. Rabe, *J. Am. Chem. Soc.* **2010**, *132*, 2104.
- 20 J. H. Jung, M. Park, S. Shinkai, *Chem. Soc. Rev.* **2010**, *39*, 4286.
- 21 Y. Okazaki, T. Buffeteau, E. Siurdyban, D. Talaga, N. Ryu, R. Yagi, E. Pouget, M. Takafuji, H. Ihara, R. Oda, *Nano Lett.* **2016**, *16*, 6411.
- 22 N. Kameta, J. Dong, H. Yui, *Small* **2018**, *14*, 1800030.
- 23 Q. Lu, Y. Kim, N. Bassim, N. Raman, G. Collins, *Analyst* **2016**, *141*, 2191.
- 24 N. Kameta, Y. Manaka, H. Akiyama, T. Shimizu, *Adv. Biosyst.* **2018**, *2*, 1700214.
- 25 N. Kameta, M. Masuda, T. Shimizu, *ACS Nano* **2012**, *6*, 5249.
- 26 N. Kameta, H. Akiyama, M. Masuda, T. Shimizu, *Chem.—Eur. J.* **2016**, *22*, 7198.
- 27 N. Kameta, H. Akiyama, *Small* **2018**, *14*, 1801967.
- 28 X. Yan, P. Zhu, J. Li, *Chem. Soc. Rev.* **2010**, *39*, 1877.
- 29 T. Shimizu, N. Kameta, W. Ding, M. Masuda, *Langmuir* **2016**, *32*, 12242.
- 30 S. Ogi, K. Sugiyasu, S. Manna, S. Samitsu, M. Takeuchi, *Nat. Chem.* **2014**, *6*, 188.
- 31 W. Zhang, W. Jin, T. Fukushima, A. Saeki, S. Seki, T. Aida, *Science* **2011**, *334*, 340.
- 32 W. Zhang, W. Jin, T. Fukushima, T. Mori, T. Aida, *J. Am. Chem. Soc.* **2015**, *137*, 13792.
- 33 X. Ma, Y. Zhang, Y. Zhang, Y. Liu, Y. Che, J. Zhao, *Angew. Chem., Int. Ed.* **2016**, *55*, 9539.
- 34 T. Itagaki, S. Kurauchi, T. Uebayashi, H. Uji, S. Kimura, *ACS Omega* **2018**, *3*, 7158.
- 35 T. Hattori, T. Itagaki, H. Uji, S. Kimura, *J. Phys. Chem. B* **2018**, *122*, 7178.
- 36 A. Desai, T. J. Mitchison, *Annu. Rev. Cell Dev. Biol.* **1997**, *13*, 83.
- 37 T. Kanzaki, Y. Horikawa, A. Makino, J. Sugiyama, S. Kimura, *Macromol. Biosci.* **2008**, *8*, 1026.
- 38 C. Hou, Q. Luo, J. Liu, L. Miao, C. Zhang, Y. Gao, X. Zhang, J. Xu, Z. Dong, J. Liu, *ACS Nano* **2012**, *6*, 8692.
- 39 C. Xu, R. Liu, A. K. Mehta, R. C. Guerrero-Ferreira, E. R. Wright, S. Dunin-Horkawicz, K. Morris, L. C. Serpell, X. Zuo, J. S. Wall, V. P. Conticello, *J. Am. Chem. Soc.* **2013**, *135*, 15565.
- 40 I. W. Hamley, *Angew. Chem., Int. Ed.* **2014**, *53*, 6866.
- 41 S. Tu, S. H. Kim, J. Joseph, D. A. Modarelli, J. R. Parquette, *J. Am. Chem. Soc.* **2011**, *133*, 19125.
- 42 S. Yagai, M. Yamauchi, A. Kobayashi, T. Karatsu, A. Kitamura, T. Ohba, Y. Kikkawa, *J. Am. Chem. Soc.* **2012**, *134*, 18205.
- 43 Y. Kim, T. Kim, M. Lee, *Polym. Chem.* **2013**, *4*, 1300.
- 44 N. Kameta, M. Masuda, T. Shimizu, *Chem.—Eur. J.* **2015**, *21*, 8832.
- 45 E. R. Blout, S. G. Linsley, *J. Am. Chem. Soc.* **1952**, *74*, 1946.
- 46 C. H. Bamford, L. Brown, E. M. Cant, A. Elliott, W. E. Hanby, B. R. Malcolm, *Nature* **1955**, *176*, 396.
- 47 F. H. C. Crick, A. Rich, *Nature* **1955**, *176*, 780.
- 48 T. Shimizu, M. Kogiso, M. Masuda, *J. Am. Chem. Soc.* **1997**, *119*, 6209.
- 49 N. Kameta, M. Masuda, H. Minamikawa, T. Shimizu, *Langmuir* **2007**, *23*, 4634.
- 50 H. Cabral, N. Nishiyama, S. Okazaki, H. Koyama, K. Kataoka, *J. Controlled Release* **2005**, *101*, 223.
- 51 H. J. Gruber, C. D. Hahn, G. Kada, C. K. Riener, G. S. Harms, W. Ahrer, T. G. Dax, H.-G. Knaus, *Bioconjugate Chem.* **2000**, *11*, 696.
- 52 N. Kameta, H. Minamikawa, M. Masuda, *Soft Matter* **2011**, *7*, 4539.